Acta Cryst. (1993). D**49**, 331–343

Structure of Apo-Azurin from *Alcaligenes denitrificans* at 1.8 Å Resolution

BY WILLIAM E. B. SHEPARD, RICHARD L. KINGSTON, BRYAN F. ANDERSON AND EDWARD N. BAKER*

Department of Chemistry and Biochemistry, Massey University, Palmerston North, New Zealand

(*Received* 29 *October* 1992; *accepted* 23 *December* 1992)

Abstract

The structure of apo-azurin from *Alcaligenes denitrificans* has been determined at high resolution by X-ray crystallography. Two separate structure analyses have been carried out, (i) on crystals obtained from solutions of apo-azurin and (ii) on crystals obtained by removal of copper from previously formed crystals of holo-azurin. Data to 1.8 Å resolution were collected from the apo-azurin crystals, by Weissenberg photography (with image plates) using synchrotron radiation and by diffractometry, and the structure was refined by restrained least-squares methods to a final R value of 0.160 for all data in the range 10.0–1.8 Å. The final model of 1954 protein atoms, 246 water molecules (66 half-weighted), four SO_4^{2-} ions, and two low-occupancy (0.13 and 0.15) Cu atoms has r.m.s. deviations of 0.012, 0.045 and 0.013 Å from standard bond lengths, angle distances and planar groups. For copper-removed azurin, data to 2.2 Å were collected by diffractometry and the structure refined by restrained least squares to a final R value of 0.158 for all data in the range 10.0–2.2 Å. The final model of 1954 protein atoms, 264 water molecules, two SO_4^{2-} ions, two low occupancy (0.18 and 0.22) metal atoms and one unidentified atom (modelled as S) has r.m.s. deviations of 0.013, 0.047 and 0.012 Å from standard bond lengths, angle distances and planar groups. The two structures are essentially identical to each other and show no significant differences from the oxidized and reduced holo-azurin structures. The ligand side chains move slightly closer together following the removal of copper, with the radius of the cavity between the three strongly binding ligands, His 46, His 117 and Cys 112, shrinking from 1.31 Å in reduced azurin to 1.24 Å in oxidized azurin and 1.16 Å in apo-azurin. There is a suggestion of increased flexibility in one of the copper-binding loops but the structure supports the view that the copper site found in holo-azurin is a stable structure, defined by the constraints of the polypeptide structure even in the absence of a bound metal ion.

* To whom correspondence should be addressed

0907-4449/93/030331-13$06.00

Introduction

Azurin is a small, single-domain electron-transfer protein of 128–129 amino-acid residues (≃14.6 kDa), found principally in denitrifying bacteria. Its function is dependent on the presence of a single type I ('blue') copper atom, which changes oxidation state between Cu^{I} and Cu^{II} during electron transfer. Azurin can therefore be grouped with other single-copper proteins such as plastocyanin, pseudoazurin, stellacyanin and amicyanin, collectively known as cupredoxins (Adman, 1985, 1991). These proteins all participate in one-electron transfer, and in their oxidized, Cu^{II}, states show the striking spectroscopic properties which are characteristic of the blue copper proteins (for reviews see Gray & Malmström, 1981; Adman, 1985, 1991).

The blue copper proteins have long been considered as classic examples of proteins where a 'rack' mechanism (Gray & Malmström, 1983) or 'entatic state' (Vallee & Williams, 1968) applies. Both concepts hold to a similar view of the nature of the relationship between the metal and the protein, *i.e.* that the metal fits into a prepared site which is determined by the structural and energetic constraints of the protein molecule. This is further believed to have functional advantages, by placing the metal in a structural and electronic state which is optimal for its particular functional role. Support for these ideas has come from an elegant series of crystallographic studies on plastocyanin (Colman, Freeman, Guss, Murata, Norris, Ramshaw & Venkatappa, 1978; Guss & Freeman, 1983; Garrett, Clingeleffer, Guss, Rogers & Freeman, 1984; Guss, Harrowell, Murata, Norris & Freeman, 1986; Church, Guss, Potter & Freeman, 1986). In particular, a structure analysis of apo-plastocyanin, at 1.9 Å resolution (Garrett, Clingeleffer, Guss, Rogers & Freeman, 1984), showed that the copper binding site was hardly changed when the copper was removed. The only significant changes appeared to be the 'flipping' of one of the two His ligands, and some increased loop flexibility near the copper site.

Azurin provides a somewhat different test, when compared with plastocyanin. The copper site is more buried, with more extensive loops above the copper

site and tighter hydrophobic packing around the one semi-exposed His ligand, His 117 (Norris, Anderson & Baker, 1983; Baker, 1988). Azurin does not undergo the pH-dependent conformational change in the copper site which occurs in plastocyanin (Guss, Harrowell, Murata, Norris & Freeman, 1986) and its copper coordination is also different from that of plastocyanin. In azurin the copper geometry is best described as trigonal planar or trigonal bipyramidal (Norris, Anderson & Baker, 1986); the Cu atom lies essentially in the plane of three strongly bound ligands, His 46, His 117 and Cys 112, with bonds of 2.0–2.2 Å, while two other atoms, the thioether S atom of Met 121 and the peptide carbonyl O atom of Gly 45, make longer approaches of approximately 3.1 Å (Fig. 1). The same geometry has been determined independently in the high-resolution structure analyses of *Alcaligenes denitrificans* azurin (Norris, Anderson & Baker, 1986; Baker, 1988) and *Pseudomonas aeruginosa* azurin (Nar, Messerschmidt, Huber, van de Kamp & Canters, 1991). In the case of plastocyanin, however, the Met S atom is closer at 2.9 Å (Guss & Freeman, 1983), and the peptide O atom much further away, at 3.8 Å, so that the geometry is most often described as distorted tetrahedral.

Crystal structure analyses of oxidized and reduced azurin, from *Alcaligenes denitrificans*, at 1.8 and 1.9 Å, respectively (Norris, Anderson & Baker, 1983; Baker, 1988; Shepard, Anderson, Lewandoski, Norris & Baker, 1990), have shown that there is minimal structural change when the oxidation state is changed, giving obvious advantages for rapid electron transfer. Here we present a structure analysis of the copper-free form of the protein, aimed at examining the extent to which the binding site is affected, if at all, by metal removal or insertion. Two analyses have been carried out. In one, copper was removed from crystals of the holo-protein, by soaking in CN (as was done for plastocyanin). In the other, the apo-protein was directly crystallized from solution; this latter analysis was considered desirable in case packing constraints in the holo-protein crystals might prevent the molecules from adopting the preferred apo-azurin structure after the removal of the metal.

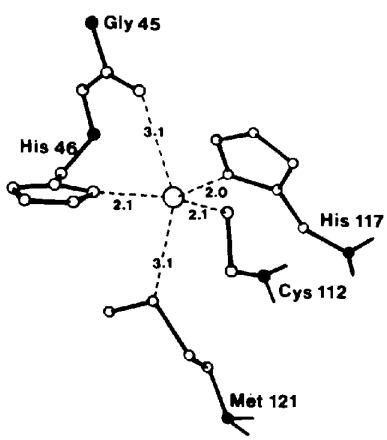

Fig. 1. Copper coordination in the oxidized holo-form of *Alcaligenes denitrificans* azurin.

Experimental

Crystal data

Azurin was extracted and purified from *Alcaligenes denitrificans* (NCTC 8582), as previously described (Norris, Anderson, Baker & Rumball, 1979). Crystals of apo-azurin were prepared in two ways. Firstly azurin was crystallized as the holo-protein, in its oxidized, copper(II), form as described by Norris, Anderson, Baker & Rumball (1979) and the copper was subsequently removed by soaking these crystals in mother liquor containing CN^-. This required soaking over a period of 3–6 months in a solution comprising 0.2 *M* potassium phosphate 75% saturated with ammonium sulfate, and 0.1 *M* KCN, at pH 7.5. The resulting colourless crystals were then returned to pH 5.5, the pH at which oxidized and reduced structures were determined (Baker, 1988; Shepard, Anderson, Lewandoski, Norris & Baker, 1990). These crystals are referred to as copper-removed azurin.

Secondly, solutions of apo-azurin were prepared by dialysing solutions of oxidized azurin in 0.18 *M* potassium phosphate against 0.1 *M* KCN at a pH of 8.0–8.5. Dialysis was carried out for 18 h, with changes every 2–4 h, until all trace of the visible blue colour had disappeared; dialysis was then continued for a further 12 h. The solution appeared free of copper as judged by its negligible absorbance at 625 nm either with or without treatment with $K_3Fe(CN)_6$. Crystals of apo-azurin were prepared by vapour diffusion, using 50–100 μl samples of apo-azurin solution, in 0.1 *M* potassium phosphate, 50% saturated with ammonium sulfate at pH 5.6–6.0; these solutions, in small open plastic tubes, were sealed in vials containing a similar solution, 70% saturated with ammonium sulfate. All crystals prepared by this method had only a very faint blue colour.

Both the apo-azurin and copper-removed azurin crystals were isomorphous with the holo-azurin crystals, having space group $C222_1$, with two molecules in the asymmetric unit and the following cell dimensions: apo-azurin $a = 75.1$, $b = 74.1$, $c = 99.5$ Å; copper-removed azurin $a = 75.1$, $b = 74.3$, $c = 99.0$ Å; *cf.* oxidized azurin $a = 75.0$, $b = 74.2$, $c = 99.6$ Å.

Data collection

A complete set of X-ray data to 1.93 Å resolution ($2\theta = 23.5$) was collected from a single apo-azurin crystal on an Enraf–Nonius CAD-4 X-ray diffractometer, equipped with a helium-filled diffracted beam path. Limited-step scan methods (Hanson, Watenpaugh, Sieker & Jensen, 1979) with profile fitting and background averaging were used, as described previously (Baker, 1988). Data were collected in shells, from high resolution to low resolution, and the 18 550 measured reflections represent approximately 92% of possible data to 1.93 Å resolution. A total of 16 593 reflections (89%) had intensities $I > 2\sigma_I$, while in the outermost shell (resolution 2.0–1.93 Å) the proportion with $I > 2\sigma_I$ was still 79%. Data were corrected for radiation damage (intensity fall-off 28% over 6 d, estimated from five standard reflections) and absorption (North, Phillips & Mathews, 1968).

A second set of apo-azurin data, to 1.8 Å resolution, was collected by screenless Weissenberg photography using a Weissenberg camera equipped with imaging plates developed by Dr N. Sakabe at the Photon Factory synchrotron radiation source, Tsukuba, Japan (Sakabe, 1991). Data were collected from two crystals, mounted about their *b* and *c* axes, respectively. In each case a rotation range exceeding 90°, and including both non-rotation axes, was covered; each image plate covered a rotation of 14°, with an overlap of 0.5 between successive plates, giving a total range of 108.5° for eight exposures. The exposure time for the recording of each image was approximately 2 min, giving each crystal a total exposure in the X-ray beam of 16 min. With a camera radius of 430 mm and X-ray wavelength of 1.0 Å, the maximum resolution was 1.8 Å. Diffraction images were processed using the program *WEIS* (Higashi, 1989). From a total of 63 360 measured reflections to 1.8 Å resolution, 18 545 unique reflections were obtained with a merging *R* value ($R = \sum |I - \bar{I}| / \sum \bar{I}$) of 0.035.

Finally, the diffractometer and synchrotron data sets were scaled and merged to give an overall data set of 24 722 reflections to 1.8 Å resolution, of which 89% had intensities $I > 2\sigma_I$ (74% with $I > 2\sigma_I$ in the highest resolution shell, 1.8–1.9 Å). The merging *R* value for the diffractometer and synchrotron data sets was 0.055.

Crystals of copper-removed azurin were smaller and more weakly diffracting (perhaps because of the prolonged soaking in CN^-) and at the time we did not have access to a synchrotron source. Therefore data were collected on a CAD-4 diffractometer, as described above, using two crystals to obtain data to a maximum resolution of 2.2 Å. This data set comprised 16 203 unique reflections of which 12 293 (76%) had intensities $I > 2\sigma_I$ (60% with $I > 2\sigma_I$ in the highest resolution shell, 2.2–2.3 Å). The overall merging *R* value for redundant data between the two crystals was 0.050.

Refinement

For both apo-azurin and copper-removed azurin the isomorphism of the crystals with those of the holo-protein implied that the latter could be used as the starting model for crystallographic refinement. Thus coordinates for the initial models were taken from the oxidized azurin structure (Baker, 1988) except that the Cu atoms, the metal-binding ligands (side chains of His 46, Cys 112, His 117 and Met 121) and all solvent molecules were removed.

Crystallographic refinement was carried out using the fast Fourier version of the restrained least-squares program *PROLSQ* (Hendrickson & Konnert, 1980). Parameters which were restrained included bond lengths, inter-bond angle distances, planar groups, non-bonded contact distances, chiral volumes and *B* factors. No non-crystallographic symmetry restraints were imposed on the two crystallographically independent molecules in the asymmetric unit. Refinement proceeded in a series of rounds, during each of which the geometrical restraints were relaxed and then tightened again. An overall *B* factor was used in the first round of refinement, after which individual *B* factors were refined, first with tight restraints, later with looser restraints. At intervals, between rounds, refinement was interrupted for manual model rebuilding on an Evans and Sutherland PS 330 interactive graphics system, using the program *FRODO* (Jones, 1978). Both $2F_o - F_c$ and $F_o - F_c$ maps were examined each time and extensive use was made of 'omit' maps to examine particular parts of the structure (the residues or solvent molecules in question were omitted from the model and refinement continued for 3–5 cycles prior to calculation of the maps in order to minimize model bias).

The course of refinement for each of the two structures is shown in Table 1. A similar strategy was used in each case. During most of the refinement the lower resolution limit for included data was 5.0 Å but this was changed to 10.0 Å towards the end. All data within the resolution range were used, with no σ cut-off. The side chains of the potential copper ligands, His 46, Cys 112, His 117 and Met 121, were built into the model after the first round of refinement cycles ($R \simeq 0.24$), and the first solvent molecules were introduced after round two ($R \simeq 0.20$). Peaks in the electron density were only interpreted as solvent molecules if their heights (in $F_o - F_c$ maps) were greater than three times the r.m.s. deviation of the map, and they occupied stereochemically reasonable positions (*i.e.* were within hydrogen-

Table 1. *Course of refinement*

Round*	*R* value	Comments
(*a*) Apoazurin		
1	0.318–0.255	5.0–1.9 Å data. Positional refinement. 1924 protein atoms. Overall *B* factor of 25 Å^2.
2	0.248–0.207	Ligand side chains added. Atomic positions, individual *B* factors refined. 1954 protein atoms.
3	0.212–0.170	Solvent molecules added. Atomic positions, individual *B* factors refined. 1954 protein atoms, 114 water.
4	0.175–0.159	Further solvent added. Atomic positions, individual *B* factors refined. 1954 protein atoms, 202 water, 4 SO_4^{2-} ions.
5	0.190–0.173	10.0–1.8 Å data. Atomic positions, individual *B* factors refined. 1954 protein atoms, 209 water, 4 SO_4^{2-} ions.
6	0.180–0.164	Model checked extensively. Further solvent added. Atomic positions, individual *B* factors refined. 1954 protein atoms, 266 water, 4 SO_4^{2-} ions.
7	0.164–0.160	Water with $B > 65$ Å^2 given occupancy = 0.5. Two Cu atoms (occupancy = 0.15) added. Atomic positions, individual *B* factors refined. 1954 protein atoms, 266 water, 4 SO_4^{2-}, 2 Cu.
8	0.165–0.162	Model checked extensively. Half-occupancy waters with $B > 65$ Å^2 removed. Full-occupancy waters with $B > 65$ Å^2 reduced to 0.5. Atomic positions, individual *B* factors refined. 1954 protein atoms, 247 water, 4 SO_4^{2-}, 2 Cu.
9	0.162–0.160	Copper occupancies refined with *TNT*. Solvent rechecked. Final refinement of atomic positions, *B* factors with *PROLSQ*. 1954 protein atoms, 247 water, 4 SO_4^{2-}, 2 Cu.
(*b*) Copper-removed azurin		
1	0.302–0.240	5.0–2.2 Å data. Positional refinement. 1924 protein atoms. Overall *B* factor 25 Å^2.
2	0.223–0.191	Ligand side chains added. Atomic positions, individual *B* factors refined. 1954 protein atoms.
3	0.195–0.164	Model checked extensively, solvent added. Atomic positions, *B* factors refined. 1954 protein atoms, 189 water, 2 SO_4^{2-}.
4	0.185–0.165	10.0–2.2 Å data. All solvent checked with 'omit' maps. Atomic positions, *B* factors refined. 1954 protein atoms, 229 water, 2 SO_4^{2-}.
5	0.175–0.163	Added further solvent. Atomic positions, *B* factors refined. 1954 protein atoms, 287 water, 2 SO_4^{2-}.
6	0.163–0.158	Model checked extensively. Termini rebuilt. All water with $B > 60$ Å^2 checked. Two Cu atoms (occupancy 0.1) added. One S atom (disordered SO_4^{2-}) added. Atomic positions, *B* factors refined. 1954 protein atoms, 264 water, 2 SO_4^{2-}, 1 S, 2 Cu.
7	0.160–0.158	Copper occupancies refined with *TNT*. All water with $B > 60$ Å^2 checked. Final refinement of atomic positions, *B* factors with *PROLSQ*. 1954 protein atoms, 264 water, 2 SO_4^{2-}, 1 S atom, 2 Cu.

* Each refinement round generally comprised 15–30 cycles in which geometrical restraints were loosened (typically to r.m.s. deviations in bond lengths of ~0.06–0.08 Å) then retightened.

bonding distance of other hydrogen-bonding groups and were not close to protein groups whose conformations were in doubt). Protein groups and solvent molecules with high *B* factors (> 50 Å^2) were omitted from the model on a number of occasions for rebuilding or checking in 'omit' maps.

Solvent molecules were initially all modelled as water molecules, with unit occupancy. Towards the end of refinement ($R \simeq 0.17$) some solvent molecules which had high *B* factors ($B > 65$ Å^2) but which consistently reappeared in 'omit' maps, were re-examined. No change was made to the lower resolution copper-removed model, but for apo-azurin these solvent molecules were given new occupancies of 0.5. On further refinement the *B* factors of a few of these continued to increase steadily, and these were removed from the model. Most, however, stabilized with *B* factors of 40–50 Å^2 and were retained in the model as half-weighted water molecules.

Sulfate ions were located in both structures (two in copper-removed azurin, four in apo-azurin). These were identified by the size and shape of their electron-density peaks (*e.g.* Fig. 2) and by their environments; in each case the site when modelled as water had no hydrogen-bonded contacts within 3.5 Å, but when modelled as SO_4^{2-} was found to have several favourable contacts, including one or more from positively charged protein groups.

Towards the end of refinement it had become apparent that in both structures some residual den-

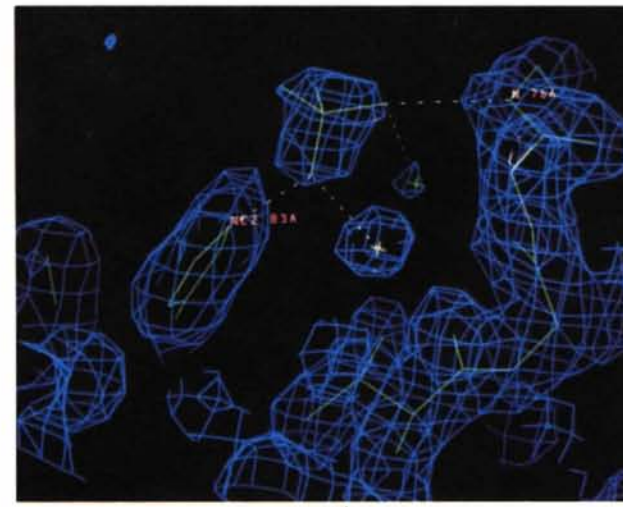

(*a*)

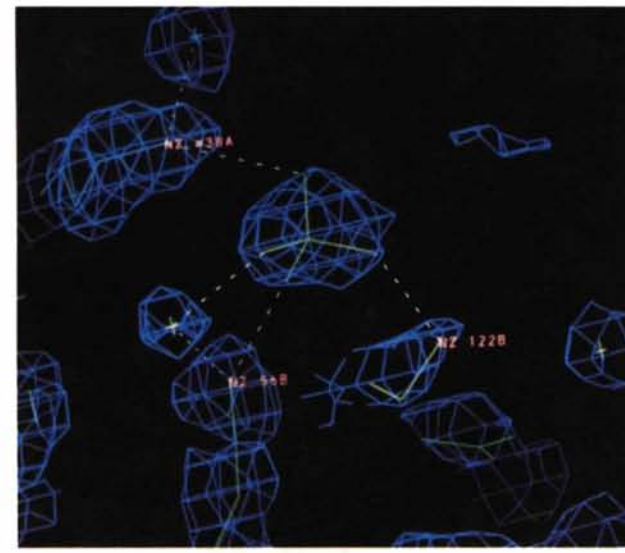

(*b*)

Fig. 2. Electron density for the two sulfate ions bound to molecule *A* of apo-azurin, taken from an omit map in which these ions did not contribute to the phasing. (*a*) The sulfate ion, which is also found in the oxidized and reduced holo-azurin structures, bound to His 83N$^{\epsilon 2}$ and Gly 76NH. (*b*) The sulfate ion bound between Lys 56 and Lys 122, with a third Lys side chain (from Lys 38 of a neighbouring molecule) and a water molecule completing the site.

sity remained at each copper site (Fig. 3). To estimate the extent of this residual density it was modelled as Cu atoms of partial occupancy. The initial occupancies were estimated by comparison with the electron density of the best-ordered water molecule in the structure (*OW* 133, attached to His117 $N^{\epsilon 2}$), as it appeared in an 'omit' map. The occupancies were then refined using the restrained least-squares program *TNT* (Tronrud, Ten Eyck & Matthews, 1987). The *B* factors of the two Cu atoms were set at values comparable with those of the surrounding protein structure while the occupancies were refined to convergence over six cycles; the occupancies were then fixed at these values and the *B* factors refined.

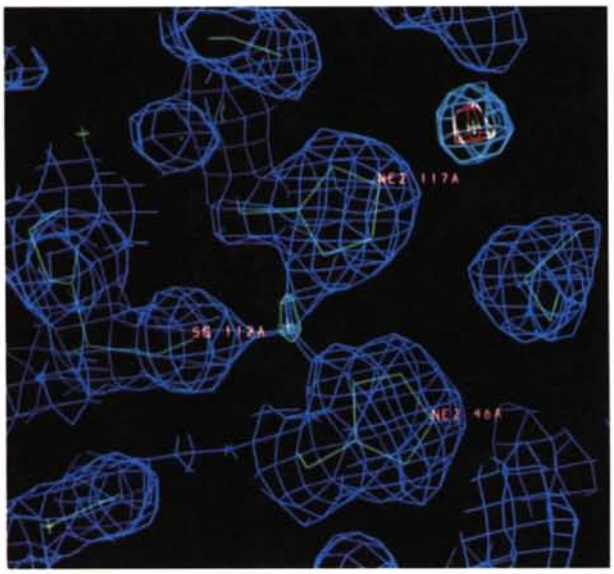

(*a*)

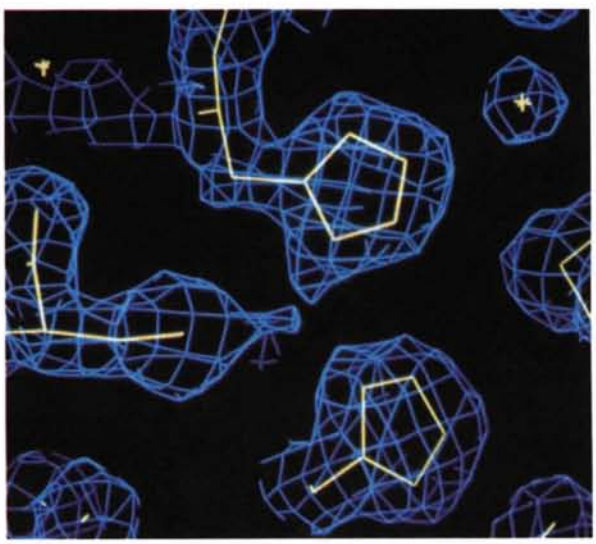

(*b*)

Fig. 3. Electron density in the binding sites of (*a*) apo-azurin and (*b*) copper-removed azurin, showing the low level of residual density at the copper position. In (*a*) the protein density is from a $2F_o - F_c$ map, contoured at a level of 1σ, while at the copper position, marked with a cross, the yellow contour is from an $F_o - F_c$ map at a level of 3σ. The level of copper density can be compared with that of the water molecule attached to His 117 $N^{\epsilon 2}$. This water molecule, previously omitted from the model is represented by contours at 3σ (yellow) and 6σ (red). In (*b*) the $2F_o - F_c$ map for copper-removed azurin is contoured at a level of 1σ.

Final models

The final model for apo-azurin comprises 1954 protein atoms (from two apo-azurin molecules), 246 water molecules (66 of them half-occupancy), four SO_4^{2-} ions and two partial-occupancy (0.13 and 0.15) Cu atoms. That for copper-removed azurin consists of 1954 protein atoms, 264 water molecules, two SO_4^{2-} ions, two partial-occupancy (0.18 and 0.22) 'Cu' atoms and one unidentified atom treated as the sulfur of a disordered SO_4^{2-}. Both protein models are constrained close to standard geometry; for apo-azurin r.m.s. deviations from standard bond lengths, angle distances and planar groups are 0.012, 0.045 and 0.013 Å, respectively, while for copper-removed azurin the corresponding values are 0.013, 0.047 and 0.012 Å. Both give excellent agreement with the observed X-ray data. For apo-azurin the final crystallographic *R* value is 0.160 for all data (22 667 reflections) in the resolution range 10.0–1.8 Å, while for copper-removed azurin $R = 0.158$ for all data (16 003 reflections) in the range 10.0–2.2 Å. The fit of the models to the final $2F_o - F_c$ electron-density maps is also excellent (see Fig. 4, and discussion below).

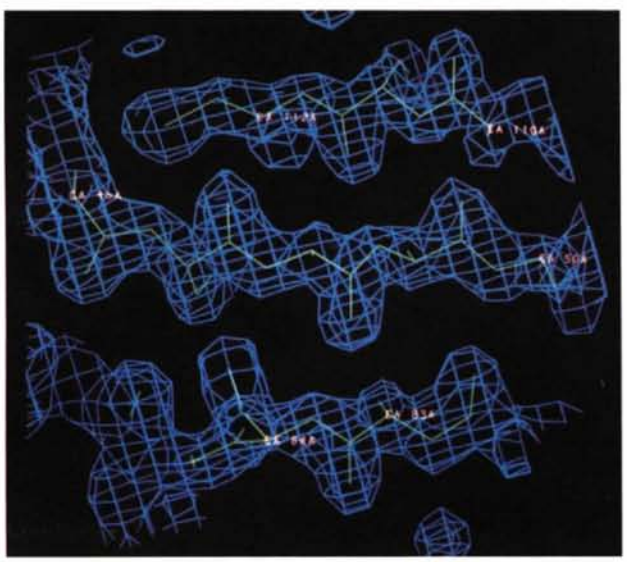

Fig. 4. Electron density for three strands of the β-sheet in the apo-azurin molecule. From a $2F_o - F_c$ map contoured at a level of 1.5σ.

The atomic coordinates for both structures have been deposited in the Brookhaven Protein Data Bank.*

Structure of apo-azurin

Quality of the models

Several different methods have been used to estimate the accuracy of the two structures. Luzzati plots (Luzzati, 1952) are consistent with average coordinate errors of 0.15 and 0.18 Å for apo-azurin and copper-removed azurin, respectively (Fig. 5*a*). As noted previously (Baker, 1988) these can be taken as maximum average errors over most of the structure, with well ordered regions (*e.g.* the binding site) being better than this and some of the loops and more mobile side chains distinctly less well defined. A σ_A plot (Read, 1986) for each structure (Fig. 5*b*) gives similar values of 0.20 and 0.27 Å.

* Atomic coordinates and structure factors for apo-azurin (Reference: 1AZB, R1AZBSF) and copper-removed azurin (Reference: 1AZC, R1AZCSF) have been deposited with the Protein Data Bank, Brookhaven National Laboratory. Free copies may be obtained through The Technical Editor, International Union of Crystallography, 5 Abbey Square, Chester CH1 2HU, England (Supplementary Publication No. SUP 37076). A list of deposited data is given at the end of this issue.

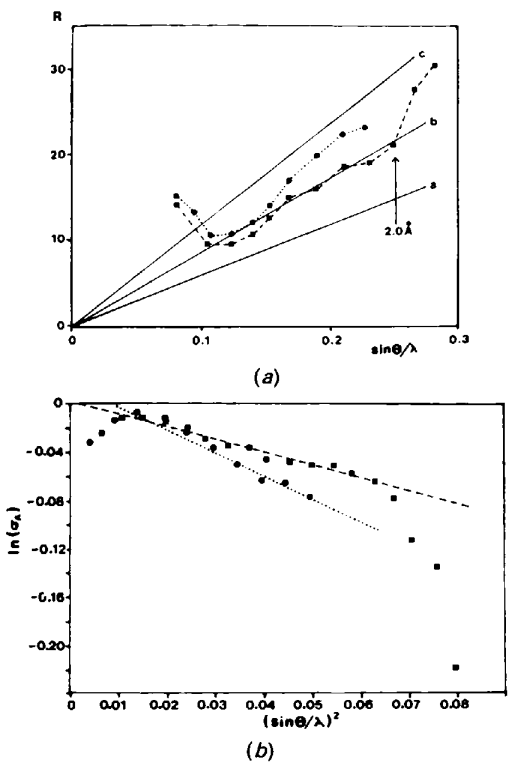

Fig. 5. Error estimates for apo-azurin (■–■) and copper-removed azurin (●·····●) structures. (*a*) Luzzati plots of R as a function of resolution with error levels shown as full lines (a = 0.10, b = 0.15, c = 0.20 Å). (*b*) σ_A plots (Read, 1986).

Table 2. *Comparisons between the two non-crystallographically related molecules of each structure*

R.m.s. deviations are given for various structural parameters.

	Apo-azurin	Copper-removed azurin
Main-chain atom positions* (Å)	0.28	0.29
Binding-site surrounds† (Å)	0.13	0.20
Binding-site residues‡ (Å)	0.12	0.15
Distances in binding site (Å)	0.06	0.10
Hydrogen-bond distances (Å)	0.10	0.16
Torsion angles§ φ ( )	6.1	6.6
ψ ( )	5.7	6.2
B factors main chain (Å²)	4.0	4.2
side chain (Å²)	4.9	4.8

* Residues 3–127 (N, C$^\alpha$, C, O atoms).
† Residues 10–12, 15, 35, 44–47, 112–117, 121 (all atoms).
‡ Residues 45, 46, 112, 117, 121 (all atoms).
§ Excluding 5% of angles with deviations greater than 3 × r.m.s. deviation.

Comparisons of the two molecules in each asymmetric unit give a further independent check of accuracy, although again these are likely to represent upper limits, as the two crystallographically independent molecules experience slightly different crystal-packing forces. Main-chain atoms (N, C$^\alpha$, C, O) can be superimposed with r.m.s. deviations of 0.28 and 0.29 Å for apo-azurin and copper-removed azurin, respectively (omitting the poorly defined N- and C-terminal residues, 1–2 and 128–129, for each molecule). Distances in the copper binding sites agree much more closely; r.m.s. deviations are 0.08 and 0.10 Å, respectively. Other measures of similarity between the two independent molecules for each structure are discussed below and summarized in Table 2.

The fit to the electron density has been quantified by calculating real-space correlation coefficients which express the fit of the model to the electron density; the method used was that in the *CCP*4 suite of programs for protein crystallography (SERC Daresbury Laboratory, 1986). For apo-azurin, at 1.8 Å resolution, 94% of residues have correlation coefficients greater than 0.8 for their main-chain atoms (73% greater than 0.9), and 63% have correlation coefficients greater than 0.8 for side-chain atoms. Only seven residues (Ala 1, Gln 2, Gln 28 and Ser 128 of molecule *A* and Ala 1, Lys 24 and Ala 40 of molecule *B*) have correlation coefficients less than 0.7 for main-chain atoms, and 15 residues (Ala 1, Ala 5, Asn 10, Lys 18, Lys 101, Ala 107 and Ala 119 of molecule *A*, and Ala 1, Thr 30, Ala 43, Lys 52, Ala 54, Thr 78, Lys 85 and Ala 107 of molecule *B*) have correlation coefficients less than 0.5 for side-chain atoms. For copper-removed azurin, at lower resolution (2.2 Å), correlation coefficients are even better.

The most poorly defined residues are identified by their high B values, and are the same in both molecules and in both structures – there is no significant

difference between the apo-azurin and copper-removed structures in this respect. Those parts of the molecule with $B > 50$ Å^2 are the N- and C-terminal residues, 1–2 and 129, and the loop 104–107, together with the side chains of Glu 4, Gln 14, Lys 18, Glu 19, Lys 27, Gln 28, Lys 52, Glu 53, Gln 57, Lys 74, Thr 78, Lys 85, Asp 98, Lys 101 and Lys 126. Almost all of these are Lys and Glx residues which project from the surface of the molecule and are clearly mobile.

Conformational angles φ and ψ agree very well between the two molecules of each structure and between structures (r.m.s. deviation 6.1° for φ and 5.7° for ψ for 95% of residues over all four molecules) and are clustered in the allowed regions of conformational space (Fig. 6). Side-chain torsion angles χ_1 are clustered around the preferred values of −60, 60 and 180°, with r.m.s. deviations from these ideal values of 13.2, 11.2 and 6.8° (overall 11.2°).

Crystal packing and non-crystallographic symmetry

Both the apo-azurin and copper-removed azurin crystal structures are isomorphous with that of oxidized azurin (maximum change in any unit-cell edge is 0.5%), and thus share the same crystal packing. This has been described in detail for oxidized azurin (Baker, 1988). In the apo-azurin and copper-removed azurin crystal structures the only intermolecular contacts which are not conserved are several involving highly mobile or disordered groups.

As for oxidized azurin, the asymmetric unit of each structure contains two molecules related by a non-crystallographic twofold axis which lies approximately along the [110] direction. The spherical polar angle rotations which relate molecule B to molecule A are: apo-azurin $\omega = 89.0$ $\varphi = 47.8$ $\chi = 179.6°$; copper-removed azurin $\omega = 88.7$ $\varphi = 48.4$ $\chi = 179.5°$; *cf.* oxidized azurin $\omega = 88.9$ $\varphi = 47.9$ $\chi = 179.7°$, where ω is the angle between the z axis and the rotation axis, φ is the angle between the y axis and the projection of the rotation axis in the xy plane, and χ is the rotation angle. The transformations that give the optimal superposition of molecule B (x_2, y_2, z_2) on molecule A (x_1, y_1, z_1) are

$$\begin{pmatrix} x_1 \\ y_1 \\ z_1 \end{pmatrix} = \begin{pmatrix} -0.09878 & 0.99495 & 0.01764 \\ 0.99469 & 0.09821 & 0.03085 \\ 0.02896 & 0.02060 & -0.99937 \end{pmatrix} \begin{pmatrix} x_2 \\ y_2 \\ z_2 \end{pmatrix} + \begin{pmatrix} 0.73842 \\ -1.06938 \\ 24.49976 \end{pmatrix}$$

for apo-azurin and

$$\begin{pmatrix} x_1 \\ y_1 \\ z_1 \end{pmatrix} = \begin{pmatrix} -0.11769 & 0.99277 & 0.02368 \\ 0.99237 & 0.11670 & 0.03971 \\ 0.03666 & 0.02818 & -0.99893 \end{pmatrix} \begin{pmatrix} x_2 \\ y_2 \\ z_2 \end{pmatrix} + \begin{pmatrix} 1.00501 \\ -1.09668 \\ 24.25116 \end{pmatrix}$$

for copper-removed azurin.

Various comparisons of the two molecules in the asymmetric unit of each structure are summarized in Table 2. Superpositions, carried out by the method of Kabsch (1978), show a similar level of agreement to that in oxidized azurin (Baker, 1988). For the polypeptide chain the agreement is poorest at the N and C termini, where the density is weak and conformations appear to differ between the two molecules, and at some of the loops between secondary structure elements (see Fig. 7). Conformational differences in the latter arise either from slight differences in lattice contacts, which affect residues 23–27 and 38–42, or simply from conformational flexibility as in the loop 103–107, which has B factors in the range 50–80 Å^2. The differences in loops are all lateral displacements rather than configurational differences, and in fact an NMR analysis of *Pseudomonas aeruginosa* azurin gives the same types of turns as are seen in the crystal structures (van de Kamp, Canters, Wijmenga, Lommen, Hilbers, Nar, Messerschmidt & Huber, 1992), even for those which have high B factors in the crystal structures.

Agreement between the two independent molecules is closer for the secondary structure elements, especially the β-structure (r.m.s. deviations 0.22 and 0.20 Å for apo-azurin and copper-removed azurin, respectively), and for residues in and around the copper sites (r.m.s. deviations 0.12–0.20 Å, see Table 2). These figures are similar to the error estimated from the X-ray data. Global superpositions are, of course, affected by any rigid-body movements of

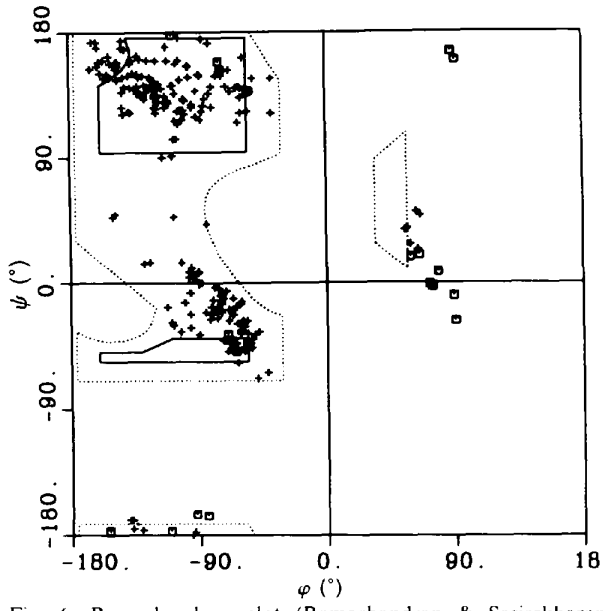

Fig. 6. Ramachandran plot (Ramachandran & Sasisekharan, 1968) for the two independent molecules of apo-azurin, with glycine residues shown as squares and all other residues as crosses.

parts of a molecule, and the accuracy of *local* structural features is more properly described by the r.m.s. deviations in hydrogen-bond lengths and non-bonded contacts, which were not significantly restrained in these refinements. For example, for apo-azurin the r.m.s. deviation for non-bonded distances in the binding site is ~0.06 Å (14 contacts < 4 Å), similar to the r.m.s. deviation in copper-ligand bond distances for oxidized azurin (0.04 Å; Baker, 1988). For the lower resolution copper-removed structure the agreement is less close (0.10 Å).

Other molecular features also agree closely. As shown in Fig. 7(*b*), the main-chain *B* factors for the two apo-azurin molecules follow each other very closely. A similar pattern is seen for copper-removed azurin. There are also no significant differences in

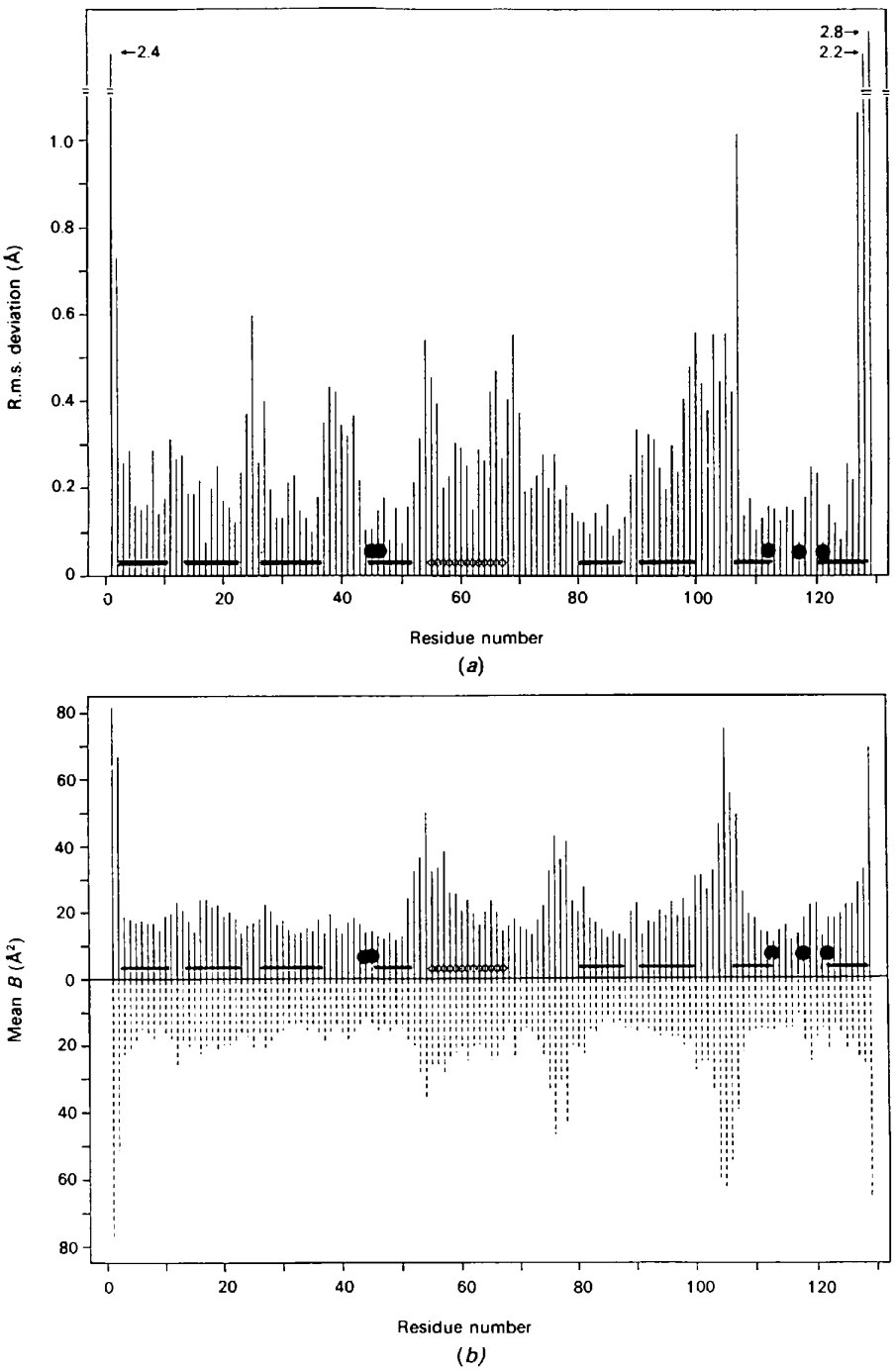

Fig. 7. Plots showing the agreement between the two independent apo-azurin molecules in the asymmetric unit, as a function of residue number. (*a*) The r.m.s. deviation in main-chain atom positions (average of N, C^{α}, C, O) after superpositions. (*b*) Average main-chain *B* factors. In both cases secondary structures are indicated ——— (β-strands) and ◇◇◇◇ (helices) and copper-binding residues (●).

Table 3. *Superpositions of apo-azurin on copper-removed, oxidized and reduced azurin structures*

Values given for molecule *A* followed by those for molecule *B*.

	R.m.s. deviations (Å) for apo-azurin		
	Cu-removed	Oxidized	Reduced
Main-chain atoms (residues 3–127)	0.16 0.15	0.17 0.14	0.20 0.19
Main-chain atoms, β-structure (residues 3–10, 14–22, 27–36, 45–51, 81–87, 91–99, 107–112, 121–127)	0.13 0.13	0.13 0.13	0.16 0.15
All atoms, Cu site surrounds (residues 10–12, 15, 35, 44–47, 112–117, 121)	0.15 0.15	0.13 0.13	0.19 0.25
All atoms, Cu site (residues 45, 46, 112, 117, 121)	0.13 0.16	0.14 0.14	0.15 0.20

main-chain torsion angles or in hydrogen bonding (except, in the latter case, for some of the more flexible, less well defined side chains).

Polypeptide-chain conformation

The overall organization of the azurin molecule has already been described in detail (Baker, 1988). The polypeptide-chain conformations of apo-azurin and copper-removed azurin are essentially identical to each other and to oxidized and reduced holo-azurins, within the accuracy of the crystallographic analyses (see Fig. 8). The electron density for the N-terminal residues, Ala 1 and Gln 2, is better for apo-azurin than for any of the other structures and their conformation in this structure is correspondingly more reliable – this is the major site of disagreement. Results of superpositions of the four structures are summarized in Table 3, with molecule *A* superimposed on molecule *A* in each case, and molecule *B* on molecule *B*, to minimize the effects of crystal-packing differences. The r.m.s. deviations are of the order of 0.12–0.15 Å for comparisons of apo-azurin with copper-removed and oxidized azurins, and slightly higher (0.16–0.18 Å) with reduced azurin. The differences are generally the same whether main-chain atoms or more restricted regions, *e.g.* the copper binding sites, are compared. Thus it is apparent that the protein structure is not significantly perturbed by the removal of the Cu atom, nor is there any difference whether the apo-protein itself is crystallized or the copper is removed from the holo-azurin crystals.

The copper binding site

Just as the polypeptide chain is left undisturbed by the removal of the metal ion, so the immediate copper binding site is also unchanged (see Fig. 9).

Fig. 8. Superposition of C^{α} plots for apo-azurin (yellow), copper-removed azurin (green), oxidized azurin (blue) and reduced azurin (purple).

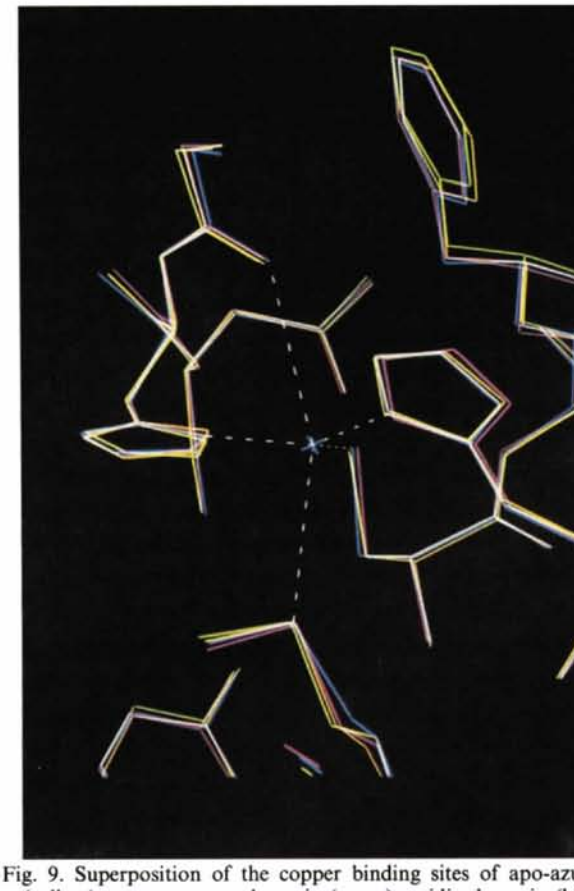

Fig. 9. Superposition of the copper binding sites of apo-azurin (yellow), copper-removed azurin (green), oxidized azurin (blue) and reduced azurin (purple). The copper position in oxidized azurin is shown with a cross.

Superpositions, either of just the metal-binding residues or of the wider copper site, show very close correspondence between the apo-azurin and oxidized azurin structures (r.m.s. deviation 0.12–0.15 Å) (see Table 3). The only change is a small inwards movement of the three equatorial copper ligands, His 46, Cys 112 and His 117, such that the distance $46N^{\delta1}\cdots117N^{\delta1}$ is reduced from 3.23 to 3.03 Å, $46N^{\delta1}\cdots112S^{\gamma}$ is reduced from 3.91 to 3.77 Å, and $112S^{\gamma}\cdots117N^{\delta1}$ is reduced from 3.57 to 3.53 Å. (These distances are averages for the two independent molecules, but in each case decreases occur for both.)

In apo-azurin the S atom of Cys 112 will be protonated, and assuming the expected tetrahedral geometry for this atom, the H atom should be directed towards the position occupied by copper in the holo-protein. The orientation is maintained by the two N—H···S hydrogen bonds, from 47NH and 114NH, which stabilize the sulfur position and maintain a tetrahedral geometry around it (Baker, 1988). The imidazole $N^{\delta1}$ lone pairs will then be directed approximately towards the H atom which could be regarded as forming a bifurcated hydrogen bond (approximate distances $46N^{\delta1}\cdots H$ 2.59 and $117N^{\delta1}\cdots H$ 2.40 Å). These interactions should help maintain the stability of the ligand arrangement in the absence of a bound metal ion.

An indication of the extent to which the metal site shrinks in apo-azurin can be obtained by calculating the radius of the cavity between the equatorial ligands His 46, His 117 and Cys 112. Using radii of 0.71 Å for nitrogen and 1.06 Å for sulfur, the radius of this central cavity is 1.16 Å in apo-azurin and 1.21 Å in copper-removed azurin, compared with 1.24 Å in oxidized azurin and 1.31 Å in reduced azurin. The value for the lower resolution copper-removed structure is the least accurate, but the others agree well between the two molecules (1.14 and 1.18 Å for apo-azurin, 1.22 and 1.25 Å for oxidized azurin, and 1.31 and 1.31 Å for reduced azurin). Thus although the differences are small, the figures indicate a steady gradation from apo- to oxidized to reduced azurin.

Other features of the binding site are as in holo-azurin. The distance between the two weak axial ligands, Gly 45O and Met $121S^{\delta}$ is hardly changed from that in oxidized azurin (5.97 compared with 5.99 Å) and the hydrogen bonds and packing interactions which fix the positions and orientations of the other ligands are also unchanged. His 46 is hydrogen bonded through $N^{\epsilon2}$ to the C=O group of Asn 10 (2.75 *cf.* 2.71 Å), His $117N^{\epsilon2}$ is hydrogen bonded to a tightly bound water molecule, 133 *OW* (2.78 *cf.* 2.72 Å) and sandwiched between the side chains of Met 13 and Phe 114, and Cys $112S^{\gamma}$ receives hydrogen bonds from the peptide NH groups of Asn 47 (3.42 *cf.* 3.49 Å) and Phe 114 (3.62 *cf.* 3.58 Å).

Table 4. *Comparisons of average main-chain B factors* (Å^2)

	Apo-azurin	Copper-removed	Oxidized
All main chain*	20.0	22.8	17.8
Residues 36–46	15.7	18.1	13.7
Residues 112–117	14.0	17.3	11.8
Residues 117–121	18.0	26.5	15.1

* Omitting residues 1–2, 103–107 and 129 from each molecule.

In both the apo-azurin and copper-removed crystal structures a small amount of residual density remains at the copper sites (Fig. 3). In the case of apo-azurin the very pale blue colour of the crystals is consistent with a low copper occupancy, estimated at 15% from difference electron density and 14% from refinement. In the case of copper-removed azurin the crystals were completely colourless and remained so even when soaked in the oxidizing agent $K_3Fe(CN)_6$, suggesting that the density could represent a low-occupancy metal other than copper, perhaps zinc or mercury. In both structures, however, the occupancy is low enough (< 20%) that it does not alter any of the structural conclusions.

B factors

The pattern of *B* factors in both structures is similar to that for oxidized azurin. The regions of the polypeptide chain with the highest *B* factors (50–80 Å^2) are the N terminus (residues 1–2), the C terminus (Asn 129), the loop 103–107 at the 'southern' end of the molecule, remote from the binding site, and parts of the 'flap' region (residues 53–54 and 75–78). Omitting residues 1–2, 103–107 and 129, the mean values of the *B* factors for the main-chain atoms are 20.0 Å^2 for apo-azurin and 22.8 Å^2 for copper-removed azurin, compared with 17.8 Å^2 for oxidized azurin (Table 4).

Considering the difficulty of comparing the absolute values of *B* factors from one structure to another, given that they are influenced by data collection and refinement protocols, there is little evidence for increased flexibility following the removal of copper. The higher mean *B* factor for copper-removed azurin could, however, result in part from disorder produced by the prolonged treatment required for copper removal from the holo-azurin crystals. The copper ligands come from two loops which connect β-strands in structure, *i.e.* Gly 45 and His 46 from the loop 36–46 joining strands 3 and 4, and Cys 112, His 117 and Met 121 from the loop 112–121 joining strands 7 and 8 (Baker, 1988). Residues 36–46 and 112–117 show no increase in *B* factors beyond the overall increase (Table 4), but residues 117–121 do show a marked increase in the copper-removed structure. NMR studies have

already indicated that this region may be rather more flexible (van de Kamp, Canters, Wijmenga, Lommen, Hilbers, Nar, Messerschmidt & Huber, 1992).

Solvent structure

The solvent model for apo-azurin has been compared with that of oxidized azurin, since both structures have been refined at similar resolution (1.8 Å). For this comparison, the two solvent models were treated in the same way. Firstly, all water molecules were sorted according to whether their closest protein atom belonged to molecule *A* or molecule *B*. Molecule *B* and its associated waters was then superimposed on molecule *A* and its waters, using protein main-chain atoms to define the transformation. Where molecule *B* water positions were within 2.0 Å of molecule *A* waters these were regarded as common to both molecules, while those which did not correspond in this way were regarded as individual to molecule *A* or molecule *B*. By these criteria the apo-azurin model contains 168 common water molecules (84 pairs) and 78 individual, compared with 184 common (92 pairs) and 97 individual for oxidized azurin.

Secondly, apo-azurin molecule *A* and its waters was superimposed on oxidized azurin molecule *A* and its waters, using the protein main-chain atoms to define the transformation, and the same procedure was repeated for the molecules *B*. This allowed the solvent models for apo-azurin and oxidized azurin, which were established completely independently by different researchers, to be compared. A total of 138 (56%) of the apo-azurin water molecules are also found in the oxidized azurin structure, using a 1.0 Å cut-off for equivalence, and it is clear from Fig. 10 that the vast majority of these (114) are water molecules which are common to the two crystallographically independent molecules of the asymmetric unit. That is, approximately 60 water molecules are found in equivalent positions in both molecules of both structures. These conserved waters tend to have relatively low *B* factors (mean 42 Å^2) and multiple protein hydrogen-bond partners.

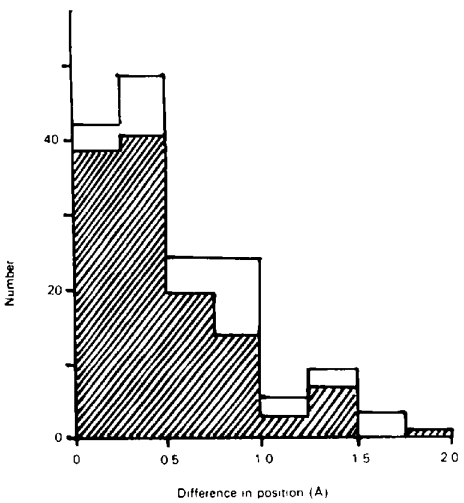

Fig. 10. Histogram showing the numbers of water molecules common to both apo-azurin and oxidized azurin structures, as a function of the differences in their positions. The shaded portion represents those which are common to both molecules of both structures.

In addition to the solvent molecules modelled as water, the apo-azurin structure contains two sulfate ions which are also found in oxidized azurin; these are bound in a shallow depression between the 'flap' and the main body of the molecule (Baker, 1988), hydrogen bonded between His 83N$^{\epsilon 2}$ and Gly 76NH, and to ordered water, on each of the two non-crystallographically related molecules. The apo-azurin structure also contains two further sulfate ions which replace apparent waters in oxidized azurin. These are found in equivalent positions on both independent molecules and are clearly sulfate ions by their density (Fig. 2) and environment; both are bound between the amino groups of Lys 56 and Lys 122, and there is an approach from a third Lys side chain (Lys 38) from a neighbouring molecule.

Discussion

The structure seen here for apo-azurin is essentially identical to that of the holo-protein (Baker, 1988), with the same polypeptide structure and minimal change in the copper binding site (movements no more than 0.1–0.2 Å). This is true irrespective of whether the apo-protein is crystallized directly or the copper is removed from previously formed crystals of the holo-protein. Thus it is consistent with the idea that the unique irregular blue copper site is defined by the constraints of the polypeptide chain, as in the related copper protein plastocyanin (Garrett, Clingeleffer, Guss, Rogers & Freeman, 1984). The copper ligands are held in place by a combination of hydrogen bonds and van der Waals interactions and the surrounding structure is the most tightly constrained, least-flexible part of the whole molecule (Baker, 1988). This structure is also maintained when different metals are bound, as for zinc (Nar, Huber, Messerschmidt, Fillipou, Barth, Jaquinod, van de Kamp & Canters, 1992) and cadmium (Baker, 1991); binding of these metals results in only small differences in the metal position and in the peptide carbonyl of Gly 45.

This apo-azurin structure does not, however, explain how copper is incorporated into the apo-protein following synthesis. In contrast to plas-

tocyanin, where the imidazole ring of His 87 (the analogue of His 117 in azurin) is rotated 180° in the apo-protein, leading to a 'revolving-door' mechanism for copper incorporation (Garrett, Clingeleffer, Guss, Rogers & Freeman, 1984), no movement is seen in the azurin binding site. The answer to this question comes from a parallel study on *Pseudomonas aeruginosa* azurin (Nar, Messerschmidt, Huber, van de Kamp & Canters, 1992). The asymmetric unit of the *P. aeruginosa* azurin crystals contains four independent molecules; in the holo-protein crystals these all have essentially identical structures, but in the apo-protein crystals the crystal packing is slightly different and two distinct structural forms are found. Two of the apo-azurin molecules have a structure similar to that seen in our study, *i.e.* closely superimposable on holo-azurin with only a slight movement of the ligand groups towards the vacated copper position. In the other two molecules, however, His 117 has swung outwards by hinging in the main-chain segment 116–118, leaving a water molecule in the copper site and some rearrangement of other neighbouring groups. This then provides a plausible model for copper incorporation.

It is apparent that (i) the structure found in holo-azurin is stable even in the absence of the metal since it is found, essentially unchanged, in *both* apo-azurin structures, but that (ii) a second form is also accessible by apo-azurin, in which His 117 is swung outwards, and which provides a mechanism for copper incorporation. Presumably an equilibrium exists in solution, as has been previously proposed (Nar, Messerschmidt, Huber, van de Kamp & Canters, 1992), although which is predominant under a particular set of conditions is difficult to know. The crystal structures give snapshots of states which are energetically accessible in solution in what must be a dynamic process.

Azurin can be seen as part of a spectrum of metalloproteins with differing degrees of constraint on their metal sites and different degrees of exposure to the outside environment. They are therefore likely to differ in the extent to which the metal site is altered by metal insertion or removal. Apart from the blue copper proteins there are now a number of other metalloproteins for which comparative crystallographic analyses have been carried out on both metal-bound and metal-free forms. These include proteins which bind zinc, as in alcohol dehydrogenase (ADH) (Schneider, Eklund, Cedergren-Zeppezauer & Zeppezauer, 1983) and carboxypeptidase A (CPA) (Rees & Lipscomb, 1983); iron, as in lactoferrin (Lf) (Anderson, Baker, Norris, Rumball & Baker, 1990) and ribonucleotide reductase (RNR) (Åberg, Nordlund & Eklund, 1992); manganese, as in concanavalin A (ConA) (Reeke, Becker & Edelman, 1978); and calcium, as in proteinase K (PRK) (Bajorath, Raghunathan, Hinricks & Saenger, 1989).

In both ADH and CPA the catalytic Zn atoms are relatively exposed in the active site, and their removal causes only very small local changes; in ADH one of the ligands, S^{γ} of Cys 46, moves 2.5 Å and the imidazole ring of His 67 rotates slightly, while in CPA a small movement of one ligand, His 196, and the nearby Glu 270, apparently allows a water molecule to occupy the site. In ConA the removal of manganese induces significant changes in the protein structure around the metal sites, although the nature of the changes has not yet been clearly defined and confirmed by high-resolution refinement. In PRK the removal of calcium causes small, concerted movements of five loops and two helices which perturb the active site some 17 Å away, and in the helix–loop–helix calcium-binding proteins (Strynadka & James, 1989) conformational change is also associated with metal binding. These binding sites all involve exposed surface loops, however, which would be expected to be more mobile than the buried, constrained site in azurin.

Both Lf and RNR have more deeply buried sites. In RNR removal of the two Fe^{3+} ions of the binuclear metal site causes the ligands to move together to form a hydrogen-bonded network, but with no other change in the protein structure (Åberg, Nordlund & Eklund, 1992). Thus this protein resembles azurin in its response. In Lf, iron removal from one site is associated with a large-scale domain movement which opens the binding cleft, but the other site remains closed even though no metal ion is bound (Anderson, Baker, Norris, Rumball & Baker, 1990). This suggests another parallel with azurin, with two conformational states (open and closed) accessible to the apo-protein.

The degree of rigidity in the metal site (or the degree to which it is pre-formed) can be related to biological function. In azurin and plastocyanin the requirements for fast electron transfer are that the metal site should undergo minimum structural reorganization (Marcus & Sutin, 1985) and a highly constrained metal site which is stable even in the absence of the metal achieves this end. In the metalloenzymes ADH, CPA and RNR the metal sites are essential to enzymatic activity and are therefore integral parts of the protein structure with defined geometrical requirements; these sites, too, change little when the metal is removed. In the calcium-binding proteins, on the other hand, conformational change accompanying metal binding is the essence of biological activity and the sites are designed accordingly.

We thank Dr Gillian Norris, who prepared the original holo-azurin crystals, and Dr N. Sakabe, for

help with data collection at the Photon Factory synchrotron source.

References

ÅBERG, A., NORDLUND, P. & EKLUND, H. (1992). *Nature (London)*, **361**, 276–278.

ADMAN, E. T. (1985). *Metalloproteins*, edited by P. HARRISON, pp. 1–42. London: Macmillan.

ADMAN, E. T. (1991). *Adv. Protein Chem.* **42**, 145–197.

ANDERSON, B. F., BAKER, H. M., NORRIS, G. E., RUMBALL, S. V. & BAKER, E. N. (1990). *Nature (London)*, **344**, 784–787.

BAJORATH, J., RAGHUNATHAN, S., HINRICKS, W. & SAENGER, W. (1989). *Nature (London)*, **337**, 481–484.

BAKER, E. N. (1988). *J. Mol. Biol.* **203**, 1071–1095.

BAKER, E. N. (1991). *J. Inorg. Biochem.* **43**, 162.

CHURCH, W. B., GUSS, J. M., POTTER, J. J. & FREEMAN, H. C. (1986). *J. Biol. Chem.* **261**, 234–237.

COLMAN, P. M., FREEMAN, H. C., GUSS, J. M., MURATA, M., NORRIS, V. A., RAMSHAW, J. A. M. & VENKATAPPA, M. P. (1978). *Nature (London)*, **272**, 319–324.

GARRETT, T. P. J., CLINGELEFFER, D. J., GUSS, J. M., ROGERS, S. J. & FREEMAN, H. C. (1984). *J. Biol. Chem.* **259**, 2822–2825.

GRAY, H. B. & MALMSTRÖM, B. G. (1981). *Copper Proteins*, edited by T. SPIRO, pp. 1–39. New York: John Wiley.

GRAY, H. B. & MALMSTRÖM, B. G. (1983). *Comments Inorg. Chem.* **2**, 203–209.

GUSS, J. M. & FREEMAN, H. C. (1983). *J. Mol. Biol.* **169**, 521–563.

GUSS, J. M., HARROWELL, P. R., MURATA, M., NORRIS, V. A. & FREEMAN, H. C. (1986). *J. Mol. Biol.* **192**, 361–387.

HANSON, J. C., WATENPAUGH, K. D., SIEKER, L. C. & JENSEN, L. H. (1979). *Acta Cryst.* A**35**, 616–621.

HENDRICKSON, W. A. & KONNERT, J. H. (1980). *Biomolecular Structure, Function, Conformation and Evolution*, Vol. 1, edited by R. SRINIVASAN, pp. 43–57. Oxford: Pergamon Press.

HIGASHI, T. (1989). *J. Appl. Cryst.* **22**, 9–18.

JONES, T. A. (1978). *J. Appl. Cryst.* **11**, 268–272.

KABSCH, W. (1978). *Acta Cryst.* A**34**, 827–828.

KAMP, M. VAN DE, CANTERS, G. W., WIJMENGA, S. S., LOMMEN, A., HILBERS, C. W., NAR, H., MESSERSCHMIDT, A. & HUBER, R. (1992). *Biochemistry*, **31**, 10194–10207.

LUZZATI, V. (1952). *Acta Cryst.* **5**, 802–810.

MARCUS, R. A. & SUTIN, N. (1985). *Biochim. Biophys. Acta*, **811**, 265–322.

NAR, H., HUBER, R., MESSERSCHMIDT, A., FILLIPOU, A. C., BARTH, M., JAQUINOD, M., VAN DE KAMP, M. & CANTERS, G. W. (1992). *Eur. J. Biochem.* **205**, 1123–1129.

NAR, H., MESSERSCHMIDT, A., HUBER, R., VAN DE KAMP, M. & CANTERS, G. W. (1991). *J. Mol. Biol.* **221**, 765–772.

NAR, H., MESSERSCHMIDT, A., HUBER, R., VAN DE KAMP, M. & CANTERS, G. W. (1992). *FEBS Lett.* **306**, 119–124.

NORRIS, G. E., ANDERSON, B. F. & BAKER, E. N. (1983). *J. Mol. Biol.* **165**, 501–521.

NORRIS, G. E., ANDERSON, B. F. & BAKER, E. N. (1986). *J. Am. Chem. Soc.* **108**, 2784–2785.

NORRIS, G. E., ANDERSON, B. F., BAKER, E. N. & RUMBALL, S. V. (1979). *J. Mol. Biol.* **135**, 309–312.

NORTH, A. C. T., PHILLIPS, D. C. & MATHEWS, F. S. (1968). *Acta Cryst.* A**24**, 351–359.

RAMACHANDRAN, G. N. & SASISEKHARAN, V. (1968). *Adv. Protein Chem.* **23**, 283–437.

READ, R. J. (1986). *Acta Cryst.* A**42**, 140–149.

REEKE, G. N., BECKER, J. W. & EDELMAN, G. M. (1978). *Proc. Natl Acad. Sci. USA*, **75**, 2286–2290.

REES, D. C. & LIPSCOMB, W. N. (1983). *Proc. Natl Acad. Sci. USA*, **80**, 7151–7154.

SAKABE, N. (1991). *Nucl. Instrum. Methods Phys. Res.* A**303**, 448–463.

SCHNEIDER, G., EKLUND, H., CEDERGREN-ZEPPEZAUER, E. & ZEPPEZAUER, M. (1983) *Proc. Natl Acad. Sci. USA*, **80**, 5289–5293.

SERC Daresbury Laboratory (1986). *CCP4. A Suite of Programs for Protein Crystallography*. SERC Daresbury Laboratory, Warrington WA4 4WD, England.

SHEPARD, W. E. B., ANDERSON, B. F., LEWANDOSKI, D. A., NORRIS, G. E. & BAKER, E. N. (1990). *J. Am. Chem. Soc.* **112**, 7817–7819.

STRYNADKA, N. C. J. & JAMES, M. N. G. (1989). *Annu. Rev. Biochem.* **58**, 951–998.

TRONRUD, D. E., TEN EYCK, L. F. & MATTHEWS, B. W. (1987). *Acta Cryst.* A**43**, 489–501.

VALLEE, B. L. & WILLIAMS, R. J. P. (1968). *Proc. Natl Acad. Sci. USA*, **59**, 498–505.